Quaternary Research (2023), **111**, 107–120
doi:10.1017/qua.2022.30

Research Article

Evidence for Pleistocene periglaciation in the lowlands of central Argentina (36–39°S)

Théa Vogt*
Friedrichstrasse 3 77694 Kehl Germany

Abstract

Pleistocene permafrost has been recognized in the lowlands of extra-Andean Argentina from Tierra del Fuego to the Rio Negro valley at 40°S, and to the Sierras Australes at 38°S. Features that could have formed only by cryogenic activity at elevations between 230–400 m above sea level in surficial deposits and in the bedrock beneath are described here as far north as 36°S. These features are not as pronounced as they are farther south because most of central Argentina was a cold desert during the glacial episodes, and therefore little ice formed. Calcareous dust, formerly considered as pedogenic and now known to be glaciogenic, is closely associated with these features. Secondary precipitates, such as lamellar crystals of calcite and gypsum, and other microscopic features like those observed in perpetually frozen ground also confirm that this region experienced permafrost at some time. These new findings mean that the area affected by periglaciation is much larger than previously thought and expanded more than 200 km farther to the north. Stratigraphic evidence and geomorphological features place both deposits and cryogenic features within them as early–middle Pleistocene age.

Keywords: Pleistocene, Periglaciation, Macrofeatures, Microfeatures, Calcareous dust, La Pampa Province, Argentina

(Received 17 May 2021; accepted 20 January 2022)

INTRODUCTION

Few published reports of past periglacial features below 500 m above sea level in Argentina are available. For instance, Corte (1967) described sand wedges in a cryoturbated gravel at Rio Gallegos in southern Patagonia (51°37'S, 20 m above sea level). Later, Liss (1969) questioned the periglacial nature of similar features observed near Puerto Madryn (42°45'S, 90 m elevation) that Corte and Beltramone (1984) proved by ^{14}C dating to have formed in permafrost during the last glacial maximum (LGM). González and Corte (1976) described a gelifluction cover and ice wedge casts penetrating the loess at González Chavez to the northeast of Bahia Blanca next to the Atlantic coast (38°S, 200 m above sea level), which they considered to be Upper Pleistocene. Corte (1983) reported 'grèzes litées' 500 m above sea level in the Sierra de la Ventana, while Czajka (1955) indicated that the northernmost border of the Pleistocene permafrost was oriented in a southwesterly direction from south of Mendoza (33°N) to the mouth of the Rio Negro (~40°S). Later, Corte (1991) traced a limit of Pleistocene permafrost from the Falkland Islands to the Andean piedmont at 40°S and northward from there to 32°S, including the Sierra de la Ventana and the Sierras Pampeanas, but excluding the eastern lowlands (Fig. 1).

Vogt et al. (2010) investigated the geomorphological evolution in the western Pampa that corresponds roughly to the La Pampa Province between 36–40°S. They found several exposures in the Pleistocene levels at ~400 m to ~200 m elevation in which the surface sediments and the bedrock beneath had been disturbed by intense cryogenic processes. To some extent this was not surprising, because periglacial features at this altitude at 40°S and near the Atlantic coast at 38–40°S had been reported and ascribed to Pleistocene permafrost by the authors noted above. However, the hypothesis of a periglacial environment in the lowlands as far north as 36°S during the Pleistocene had never been addressed. Features found in the field and results of analyses of sediments and minerals in samples from a large area of La Pampa Province are shown and discussed below, bringing a new perspective to what has been previously known.

GEOLOGICAL AND GEOMORPHOLOGICAL BACKGROUND

The study region extends ~400 km from north to south and 400 km from west to east (Fig. 1), covering the eastern foreland of the Andes chain between 36–40°S. Most of its surface consists of a plateau that falls gently eastwards from ~400 m to ~230 m above sea level with an overall slope of 0.2%. The study region is limited on its eastern side by a north-south fault scarp 50–150 m high, at the foot of which extends the subsiding Pampa Deprimida plain at 120–150 m above sea level, with numerous depressions below 100 m. It is dissected to 80–100 m above sea level by several valleys running from west to east that were triggered by subsidence of the Pampa Deprimida. The plain of the Chadileuvú-Curacó rivers at 200 m above sea level is its western limit, and the Colorado River valley at 100 m above sea level is its southern boundary. The eastern Sub–Andean piedmont begins

*Corresponding author at: Friedrichstrasse 3 D-77694 Kehl. E-mail address:<thea.vogt@gmail.com> (T. Vogt).

Cite this article: Vogt T (2023). Evidence for Pleistocene periglaciation in the lowlands of central Argentina (36–39°S). *Quaternary Research* **111**, 107–120. https://doi.org/10.1017/qua.2022.30

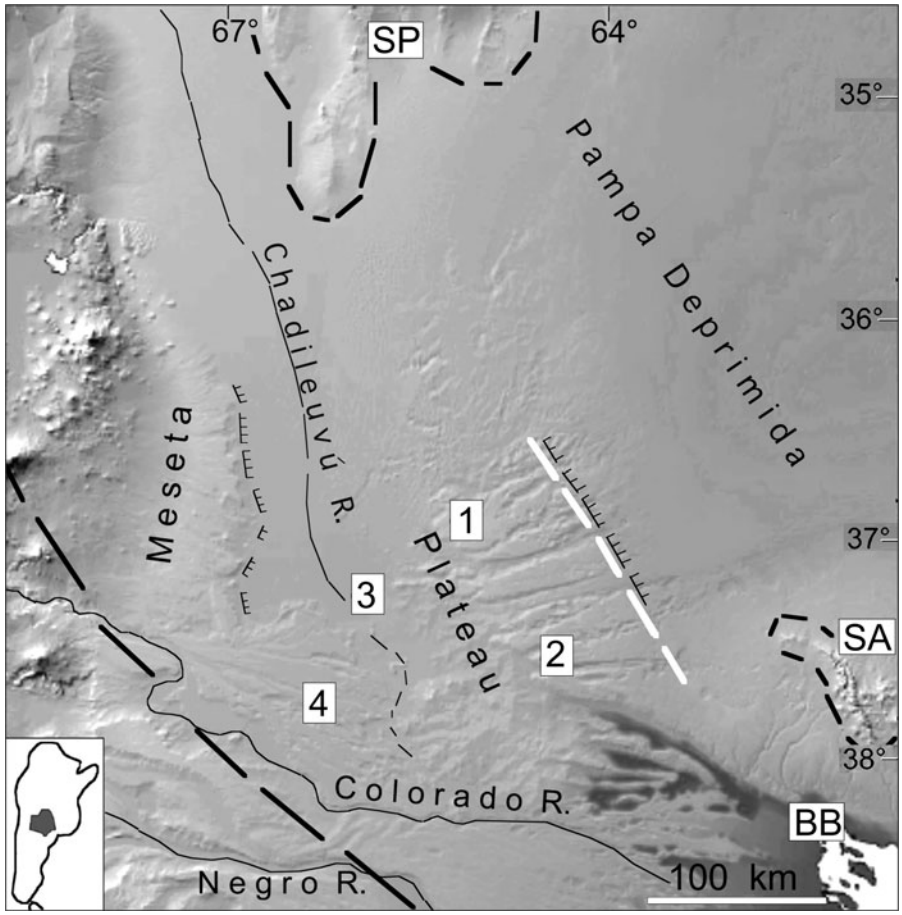

Figure 1. Radar (ERS-1 SAR) image of the La Pampa region. SP = Sierras Pampeanas; SA = Sierras Australes; BB = Bahia Blanca; 1 = exposure on the upper surface of the plateau (Valle de Chapalcó); 2 = exposure in the Valle de Hucal; 3 = exposure at Carapacha Chica; 4 = exposure on a terrace of the Rio Colorado. The black dashed line indicates the limit of the Pleistocene permafrost as sketched by Corte (1991). The white dashed line indicates the limit of permafrost as proposed here; its prolongation toward the NW would reach the SP, where permafrost was recognized. The black barbed lines indicate the western and eastern fault scarps. The insert at the lower left corner locates the La Pampa Province in Argentina.

to the west of the Chadileuvú plain, beyond the regional boundaries (Fig. 2).

Calmels and Casadío (2004) compiled an account of the regional geology, and Vogt et al. (2010) established its post-Miocene geomorphological evolution. In summary, the Plateau represents the southernmost portion of the Brazilian shield and was the divide between the Atlantic and Pacific oceans before the Andean uplift. It is underlain by metamorphic and intrusive rocks (granites and diorites), while Paleozoic and Permo-Triassic sedimentary rocks crop out at its western and southern margins.

Uplift of the Andes created a wide piedmont—an inclined plane descending east-to-southeastward from 750–700 m to ~400 m with an average gradient of 0.45%. It included the

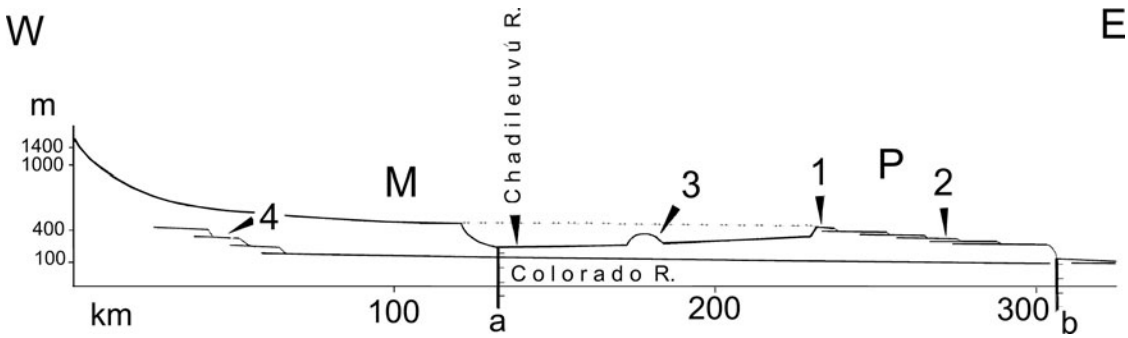

Figure 2. Diagrammatic sketch of the topography from west to east, from the piedmont to the plain: M = Basaltic meseta; P = Plateau. The dotted line restores the profile of the Sub-Andean piedmont before the graben of the Río Chadileuvú subsided. The arrows point the sites of exposures: 1 = highest level at ~400 m; 2 = intermediate level at ~260 m; 3 = Carapacha Chica; 4 = terrace of the Colorado River at ~300 m. Fault scarps limit the Basaltic meseta (a) to the west and the Plateau (b) to the east.

https://doi.org/10.1017/qua.2022.30 Published online by Cambridge University Press

Plateau and reached the Pampa Deprimida plain beyond the present eastern fault scarp. A material called "Formación Cerro Azul" by Linares et al. (1980), which consists of fine-grained sand and silt, at least 200 m thick, and more or less consolidated as siltites, blanketed the region during the Late Miocene. Despite abundant hydrogeological drilling, much of which reached the basement, no map exists of the topography under these siltites, which probably obliterated the ground unevenness. Bernardi et al. (2019) studied in detail basalt flows 4–8 m thick to the west of the Chadileuvú plain that covered the piedmont during the Pliocene and Pleistocene. The piedmont is known as the 'Meseta basáltica' (Basaltic meseta).

Apparently no additional tectonic uplift of the basement has occurred since that time, as illustrated by the topographic profile (Fig. 2). Tectonic reactivation at some time during the middle Pleistocene and before the late Pleistocene led to subsidence of the Chadileuvú graben and created the present plain. The western fault cut and displaced a basalt tongue, which is dated at 0.40 ± 0.10 Ma (Melchor and Casadío, 1999), that detached the plateau from its roots. Subsidence of the Pampa Deprimida created a fault scarp >100 m high, which limits the plateau to the east (Vogt et al., 2010).

During glacial episodes, streams flowing from the Andes Mountains crossed the Basaltic meseta and carried alluvium that covered the entire plateau. The flows concentrated during the interglacials and gradually cut into underlying alluvium, Miocene siltites, and even into the basement in some places. The result is a set of at least five stepped levels, the highest of which is ~400 m above sea level and the lowest at 230 m above sea level (Vogt et al., 2010). The deposits contain no organic remains that can be dated by ^{14}C radiometry, but their age and ages of the levels may be inferred from the following: (1) presence of basalt debris in the deposits implies that they are no older than the basalt flows (i.e., no older than Plio-Pleistocene); (2) whereas the siltites are free of carbonate, all the overlying deposits contain glaciogenic calcareous dust, as do most periglacial Pleistocene deposits in Argentina (Techer et al., 2014; Vogt et al., 2018); and (3) all deposits ascribed to the Upper Pleistocene in the region by Tapia (1935), Casadío and Schulz (1986), and Calmels et al. (1996) crop out at the bottoms of valleys and consist only of local material, mostly reworked siltites, which confirms the end of the connection between the Plateau and the piedmont. It follows that the stepped levels formed before subsidence of the Chadileuvú plain and before the late Pleistocene, and that they are most likely of early to middle Pleistocene age (Vogt et al., 2010).

CENTRAL ARGENTINA DURING THE GLACIAL EPISODES

The climate of southern and central Argentina has two major controls: the Andean chain to the west and the proximity of Antarctica to the south. The Andes lie transverse to the Southern Hemisphere westerlies and to their east cause one of the strongest orographic rain shadows on earth (Blisniuk et al., 2005). Their uplift dates back to Late Cretaceous (Ghiglione et al., 2016; Colwyn et al., 2019) and they rose rapidly after the Middle Miocene (ca. 15 Ma), strengthening the rain-shadow effect (Ramos and Ghiglione, 2008) and creating the "Arid Diagonal" of southern South America from the Atacama Desert to the dry steppes of Patagonia (Rech et al., 2010; Le Roux, 2012b; Ghiglione et al., 2016).

The onset of Antarctic glaciations dates back to the mid-Tertiary (Ingólfsson, 2004), and the cooler temperatures enhanced regional aridity. By the early Oligocene, Antarctic ice sheets were ~25% larger than now, and their growth was accompanied by a sea level that was ~105 m lower than present day (Katz et al., 2008). The glaciations first affected East Antarctica, after which a continental-sized ice sheet was developed in the earliest Oligocene (Barron et al., 1991; Isla and Espinosa, 1995; Ivany et al., 2005; Levitan and Leichenkov, 2014). The ice sheets expanded during the Middle Miocene glaciation (ca. 16.5–13 Ma), mainly at the boundary between the Middle and Late Miocene, and they became permanent from then on (Holbourn et al., 2013). The cold Falkland, or Malvinas, Current was established after the Middle Miocene (Le Roux, 2012a).

The atmospheric Antarctic Polar Front, currently near Tierra del Fuego at ~60°S, shifted ~5–6° northward following the glacial expansion (Paskoff, 1967; Caviedes and Paskoff, 1975; Clapperton, 1994), although Becquey and Gersonde (2002) estimated it to be as much as 7° northward. García et al. (2012) reckoned that the Antarctic Polar Front reached as far north as latitude 51°S, and MARGO (2009) even farther north to 45°S. These shifts caused cooling of the ocean surface water, with estimates by several authors as follows: a decrease of 4–6°C (Kaiser et al., 2005); a drop of 4.0 ± 0.8°C and temperatures of −4°C to −8°C at 60–45°S during the LGM (Annan and Hargreaves, 2013) and of 5–8°C near the continent (Hulton et al., 2002), where the mean annual temperature was ~7–8° lower than at present (Benn and Clapperton, 2000).

Tzedakis et al. (1997), however, showed that marine oxygen isotope records do not account correctly for variations on the continent. Kohfeld and Harrison (2001) considered that atmospheric models have underestimated the magnitude of cooling and drying of most of the land surface during the LGM. These huge changes had large effects on the global climate. They induced increased temperature gradients and wind strengthening, as well as continental aridification (Flower and Kennett, 1994; Haywood et al., 2009; McClymont et al., 2016). The westerlies moved farther north.

West Antarctica and its peninsula are the nearest part of Antarctica to southern Argentina and, therefore, have the greatest influence on Argentina's climate, with glacial and non-glacial periods alternating on the Peninsula. On Seymour Island, for instance, glacial deposits indicate that ice was present there at the Eocene/Oligocene boundary (Francis et al., 2009) and grounded ice reached sea level. A new glaciation followed in the late Oligocene and another in the earliest Miocene (Barker, 2007; Dingle and Lavelle, 2017). The ice cover extended during the Middle and Late Miocene with shelf-wide grounding events (Chow and Bart, 2003; Bart et al., 2005; Passchier et al., 2011) and full glaciation of the Peninsula (Coronato et al., 2004). The extension of Antarctic ice was at its maximum towards the end of the Miocene, with grounded ice extending in the Ross Sea 100 km farther northward than now (Flohn, 1988).

The present position of Antarctic sea ice is 70–60°S, while it expanded to 60–48°S during the LGM, and probably during the Late Miocene, which doubled its surface (Crosta et al., 1998; Guilderson et al., 2000; Crosta, 2009; Violante et al., 2014). The periglacial regions were not only larger in extent, they also were drier than the driest present-day periglacial regions because of drier air. The ice-free regions suffered a harsh cold climate, and permafrost formed near sea level in Patagonia (Benn and Clapperton, 2000). Permafrost still occurs on the South Shetland Islands at 25 m above sea level (López-Martínez and Serrano, 2005; López-Martínez et al., 2016). The nearby lowlands between 40–36°S could not have escaped the effects of those

https://doi.org/10.1017/qua.2022.30 Published online by Cambridge University Press

conditions, therefore a desertic periglacial environment north of 40°S seems likely.

Both enlargement of the polar ice cap and the 100–150 m sea level drop below its current level (Guilderson et al., 2000; Cavallotto et al., 2011; Violante et al., 2014) diminished the sea's surface area and hence evaporation, which in turn favored expansion of desertic land. The shoreline shifted at least 700 km eastward, which caused the climate to become increasingly continental. Sea level fell by 100–140 m during the maximum of each glacial episode (Rabassa et al., 2005; Rabassa, 2008). Consequently, much of the Argentinean continental shelf, which represents one of the largest and smoothest siliciclastic shelfs in the world (Violante et al., 2014), was exposed. Cooling of the oceans caused replacement of carbonate sediment-forming species by siliceous organisms, which explains the shelf's siliceous nature (Cortese et al., 2004). Such biogenic silica at the Polar Front accumulated fastest from 11–9 Ma (Levitan and Leichenkov, 2014). The emerged shelf was a marginal desert (Ochsenius, 1985), and much of Argentina was a cold desert during glacial times (Iriondo and Kröhling, 1995).

In dry cold climates with strong diurnal thermal excursions, rocks and mineral grains undergo a comminution to the 50–10 µm silt size (Konishchev, 1982). Quartz is the most fragile because its thermal expansion is twice that of either plagioclase or biotite (Elliott, 2006). Quartz crystals contain microfissures, ~1–10 µm wide, that facilitate disintegration to particles as small as 1 µm, which can be considered to be the limiting size of solid particles (Schwamborn et al., 2012). Such fine silt is easily picked up and carried away by wind.

Late Miocene sediments

Silts of the Cerro Azul Formation derive on one side from the barren emerged shelf, which represented an important source for wind-transported silt during glacial periods (Walter et al., 2000), and on the other side from deflation of the granular detritus of barren rocks. Strong southeasterly winds swept over the barren shelf and Sub-Andean slopes and deposited the silt on the piedmont and the Plateau. This situation lasted for several million years, which is one reason for the thickness of the deposits. Based on paleontological data, Verzi et al. (1991) concluded that the landscape was an open steppe. There were no rivers, and only episodic surficial runoff reworked the silt. Globular siliceous concretions, 10 cm or more in diameter, occur within the sediment. These form in marshes. Numerous elongated and vertically aligned concretions that lack the radial internal structure specific to rhizo-concretions that are typical of woodlands (Retallack, 2019) also are present. These concretions resulted from preferential circulation of water within retraction fissures in palustrine conditions (Giai and Tullio, 1998). Layers of salt and gypsum are also interbedded in them. The palustrine features, the slightly siliceous cementation of the sediment, and the interbedded salt and gypsum layers cannot be explained other than by the presence of a water table. Zavala and Freije (2001) ascribed to groundwater the palustrine facies within the aeolian Rio Negro Formation (Late Miocene–Early Pliocene) in nearby Patagonia.

The cold and dry climate and the consequent sparse vegetal cover allowed thermoclastic granular degradation of barren rock surfaces and the strong wind to pick up sand and silt. The limited porosity of volcanic rocks makes them resistant to frost action and therefore not subjected to spalling (Tricart, 1967). Nevertheless, the Rio Negro Formation is dominantly composed of volcanic grains, which give it a peculiar bluish color. The significant fine-grain fraction of the sediments indicates a long, strong thermal excursion and thermoclasty.

Start of glaciations in Central Argentina

The final uplift of the Patagonian Andes during the Late Miocene (Ramos and Ghiglione, 2008) combined with temperature cooling and expansion of Antarctic ice (Mercer and Sutter, 1982; Clapperton, 1993; Ton-That et al., 1999; Griffing et al., 2012; Le Roux, 2012b) led to the formation of alpine glaciers in southern Argentina during the Middle–Late Miocene (Wenzens, 2006; Glasser and Jansson, 2008; Moeller et al., 2010; Christeleit et al., 2017; Willett et al., 2020). The Patagonian Andes were covered by a continuous mountain ice sheet from 37°S to Cape Horn (56°S) (Rabassa et al., 2011). Rabassa et al. (2005) reported at least eight glacial episodes from the Middle to the Late Pliocene in addition to the Great Patagonian Glaciation (GPG) from 1.17–1.02 million years ago. The onset of glaciers resulted in powerful rivers transporting and depositing large amounts of coarse material, such as the glacio-fluvial "rodados patagónicos" (the "Patagonian Gravel Formation" of Clapperton, 1993). The effect of glaciation extended throughout all of Patagonia, as well as the Pampas (Rabassa et al., 2011). The glacial activity generated calcareous dust (20–70% $CaCO_3$) found with Pleistocene deposits in Argentina from southernmost Patagonia to at least the Mendoza Precordillera (Techer et al., 2014; Vogt et al., 2018).

The glacial periods in the western Pampa

How the glaciations progressed in the eastern portion of Central Andes between 40–36°S is not known. No investigations of the geomorphological evolution west of the Chadileuvú depression are available (Glasser and Jansson, 2008, reported remote-sensing observations only). Lliboutry (1956) established the current glacial equilibrium line on both sides of the boundary between Chile and Argentina. It runs southwards from a height of 5500–4500 m in the subtropics north of 33°S to 2500 m at 36°S, dropping slowly to 1000 m at ~48°S. Obviously, this line was lower during the glaciations. Viers (1965), who briefly explored the Andes of Mendoza between 33–35°S, observed some glaciers in the upper Colorado Basin at the foot of the Cerro Risco Plateado (34°55'S, ~4500 m above sea level), and estimated their area to be 40–50 km^2. Viers (1965) also reported several old glacier valleys and moraines, and noted the crest line hemmed by glaciers all along the full length of 20 km between Paso de las Damas (34°54'S, 3680 m above sea level) and Cerro de Santa Elena (35°07'S, 2940 m above sea level). All glaciers occurred on the east- and southeast-facing slopes. The morphometry of this upper basin (Aumassanne et al., 2018) does not reveal anything about the shape of the valleys and their glacial or fluvial nature, or the occurrence of terraces and moraines—in sum, nothing helpful for understanding the evolution of the course of one of the greatest rivers of Argentina.

The Colorado River entered the region during the Late Pliocene (Melchor and Casadío, 1999) and built a set of fluvial terraces 200 km or more long and ~100 km wide that descend in steps from 440–100 m above sea level (Vogt et al., 2010). The river cut a gorge through the basalts of the Sierra de Chachahuén (dated at 2.07 ± 0.11 Ma and 1.23 ± 0.17 Ma) and the Sierra Auca Mahuida (dated at 1.78 ± 0.1 Ma, 1.55 ± 0.07 Ma, 1.39 ± 0.14 Ma, and 0.99 ± 0.04 Ma) (Kay et al., 2006). The highest terrace at 440 m contains no volcanic minerals, and is therefore older than 2 Ma, the gorge being epigenic. Each terrace consists of homogeneous, well-layered and well-worn gravel and

https://doi.org/10.1017/qua.2022.30 Published online by Cambridge University Press

sand lenses 10 m thick with a slope of 0.1%, which is inconsistent with the previous interpretations of Melchor and Casadío (1999) of this deposit being an alluvial fan. Unfortunately, a thorough study (morphometry, morphoscopy, petrography) of the gravels and sand is lacking.

While the features of the river valley upstream of the gorges have yet to be described in detail, the occurrence of large volumes of coarse material suggests strong currents that were likely fed by large amounts of snow and ice melt. If the present glacial equilibrium line is at 2500 m to the south of 36°S, then one can infer that glaciers existed on the Andean chain at this latitude during glacial episodes.

The Pleistocene deposits

The comparison between the current climatic conditions both in La Pampa and in the unglaciated portions of Antarctica allows an estimate of the climate during the glacial episodes. The current mean annual temperature varies between 18°C and 14°C in the north and south of La Pampa, respectively, while that of Northern Patagonia (at Trelew) is ∼13°C. In contrast, temperatures of interior Antarctica (Bockheim and Tarnocai, 1998) are −18 to −20°C now, and were colder during the glacial episodes. Ice-wedge formation requires temperatures of −5°C (Washburn, 1980) or lower. The presence of ice wedge casts in Patagonia indicates a minimum temperature drop of at least 18°C to reach the −5°C threshold, which implies a north to south temperature gradient from 0°C to −4°C across La Pampa. Even though Antarctica is a useful analog, La Pampa has higher solar radiation due to its latitude (36–40°S), and consequently a greater evaporation and stronger daily thermal excursion. These factors explain La Pampa's desert environment, the intense disaggregation and cracking of the bare ground, and the nature of sediments and their post-depositional features.

Streams that built the alluvial levels transported mostly sand, but also included clasts from substrate, fragmented siltites, and debris of Paleozoic rocks. The sequenc is much the same for all levels, from bottom to top is as follows: (1) bedrock consisting of siltites and in some places of Paleozoic substrate; (2) unconformable alluvium at least 2 m thick consisting of sand, gravel, and silt, either mixed or well layered; (3) a gradual transition from siltites to overlying deposits with perturbed layering, shattering of the bedrock, mixing of silt and reworked concretions, and calcareous dust either incorporated in the alluvium and mixed with the fine matrix or in pockets and thin layers; (4) an erosional contact marked by clasts and grit where granite or other Paleozoic rocks crop out; and (5) uncemented material at the base, hardening upwards to duricrust several decimeters to >1 m thick, generally sandy and locally conglomeratic, with 25% $CaCO_3$ at the most. Several studies (Buschiazzo et al., 1987; Lorenz, 2002; Mehl and Zárate, 2007; Folguera and Zárate, 2009; Gutiérrez et al., 2019) called this material calcrete, even though there were no analytical data. However, microscopic analyses of thin sections by Vogt et al. (2002) show that the duricrust is in fact a siliceous sandstone with opal as the primary cement.

The change in the dynamics is abrupt between the aeolian siltites and the overlying stream-flow deposits. Furthermore, two characteristics differentiate the Pleistocene deposits from older ones: the shattering (clasts and angular sand grains) and the presence of calcareous dust. While the geomorphological evolution of the uphill Andean slope is poorly constrained, it can reasonably be assumed that there would have been glaciers above 2000 m during the last glacial periods. Even if there were no glaciers, there was certainly enough snow to feed the energetic and abundant currents that were able to remove and transport large loads of material. The generally clear stratification of the sediments means that they were not deposited in turbulent runoff. Furthermore, the absence of incised channels suggests that the water spread out over the frozen ground.

Thermoclastic granular disaggregation on barren rocks can explain why the mountainous slope did not supply detrital grains coarser than sand. Also, because basalt is non-frost susceptible, the abundance of basalt grains in the sediment is consistent with strong thermal excursions. The analysis of some exposures may provide an understanding of which environment produced these features.

ANALYTICAL METHODS

Numerous exposures on and outside the Plateau were studied. The aim was to explain the origin of the sediments and any post-sedimentary evolution. Grain-size distributions of the sand fraction were determined by dry sieving. The surface features of the mineral grains were observed under a stereoscopic magnifier with incident light. Minerals were identified by Scanning Electron Microscope, X-Ray Diffractometry, and Transmission Electron Microscopy (TEM, Philips EM300, 100 KV). Minerals were analyzed chemically by an analytical electron microscope (Philips CM12). Duricrusts and Miocene siltites were observed in thin sections and by SEM. The volumetric proportion of $CaCO_3$ was determined by a standard procedure with a Bernard calcimeter. Strontium, oxygen, and carbon isotopic compositions and the rare earth elemental (REE) distribution of the dust were analyzed using methods detailed in Techer et al. (2014).

FIELD OBSERVATIONS

Whatever the level, the alluvium that is spread over the plateau yields similar characteristics at both macroscopic and microscopic scales. The sequence exposes from bottom to top: (1) a bedrock of pink siltites horizontally layered with a loess-like structure and globular or elongated siliceous concretions, with outcrops of the Paleozoic substrate in some places; and (2) an unconformable alluvium at least 2 m thick consisting of sand, silt, and gravel, either mixed or well bedded, with a gradual transition from siltites to the overlying deposits. The substrate has lost its structure, is split into clasts, and consists in a mixture of silt and reworked concretions. In some places the originally pink color has turned yellowish or brown-red. Where granitic or other Paleozoic rocks crop out, the transition is an erosional contact marked by clasts and grit. Dust consisting of 20–70% CaCO3 is incorporated in the alluvium, either mixed with the fine matrix or in pockets and thin layers. A hard duricrust caps the deposits.

This common sequence shows that depositional episodes ended with strong desiccation (duricrust). The coarse material derives from substrate (i.e., shattered bedrock, siliceous concretions, intraclasts, and clasts from older duricrusts with occasional roundness that either is original for the concretions or due to cortications [= oncolites]). The sandy fraction is the same everywhere, consisting of a mixture of coarse angular grains and medium–fine, well-worn shiny grains. The coarse fraction contains sand-sized basalt grains and centimeter-sized basalt debris. Olivine grains account for as much as 45% of the >400 µm fraction. There are no visible traces of chemical weathering; rather, it seems that fragmentation was caused by long-lasting thermal stress.

https://doi.org/10.1017/qua.2022.30 Published online by Cambridge University Press

Field exposures

Two exposures of the alluvial cover are described in detail—one in the uppermost level at 415–380 m above sea level and the other in the intermediate level of 270–260 m above sea level. As noted above, the precise age of the levels is not known, but the upper level is probably early Pleistocene; the lower one is much younger according to the geomorphological framework. An exposure of Carapacha Chica at 260 m above sea level, and another in an embankment on a terrace of the Colorado River at 300 m, also were examined.

The uppermost level

The highest level, which extends from ~36°50' to 37°10'S to the north of the Valle de Chapalcó (Fig. 1, site 1; Fig. 2, site 1; Fig. 3a, b), falls gently eastwards with slope of 0.1% and is mantled entirely by alluvium and capped by a duricrust. The road cuttings along Ruta Provincial 13 (RP13) expose the deposit with the same upwards sequence everywhere: (1) Late Miocene siltites at the bottom; (2) above, at least 1 m of sandy silt with on average 40–45% of particles in the size range 50–2 μm and 7–8% particles ≤2 μm derived from the substrate and containing reworked concretions, polyhedra with facets and Fe-Mn cutans, aggregates, granules, decimeter-sized clasts of siltites, clusters of clasts, mixed with allochthonous sand and $CaCO_3$ dust (up to 30% in places); and (3) a 50–100 cm thick conglomeratic or sandy duricrust with a platy structure, <25% $CaCO_3$, folded in places (Fig. 3c). The 630–800 μm fraction is composed of 25–30% quartz grains. They are wind abraded, their size shows that they are local, and their shape indicates that they experienced long-lasting aeolian activity. The 500–100 μm sand grains are well worn and shiny, which is characteristic of fluvial transport.

The deposits show contraction features, involutions, and locally septarian-like structures. The siltites are broken into decimeter-size clasts.

The intermediate level

On the south-facing slope of the Valle de Hucal (64°23'–64°14'W; 37°78'–37°47'S; Fig. 1, site 2; Fig. 2, site 2; Fig. 4a–c), several exposures ~3 m high along the path between provincial roads RP11 and RP9 show the following sequence from bottom to top: (1) siltite; (2) ~1 m of sandy silt (24–40% of particles 50–2 μm; 6% of particles <2 μm in diameter), siltite clasts, and concretions, all reworked from the substrate, together with calcareous dust in fine layers and pockets; and (3) a platy duricrust >1 m thick consisting of hard cemented sand. The proportion of $CaCO_3$ ranges between 27–71% in the pockets, compared to only 0.5% in the duricrust.

The alluvium above the siltite has lost its original layering and is cross-cut by contraction cracks. The coarse material is aligned vertically or sub-vertically along the lineaments or forms nests (Fig. 1, site 2; Fig. 2, site b; Fig. 4a–c). The cracks are not due to desiccation because the material is too heterogeneous and consists of <50% silt and clay. There has been no compressional tectonic activity in this area since deposition, and the origin of the cracks needs to be discussed. The material is too hard for the bioturbation process suggested by Silva Nieto et al. (2017). Similar structures occur in the nearby Valles Maracó Grande and Maracó Chico.

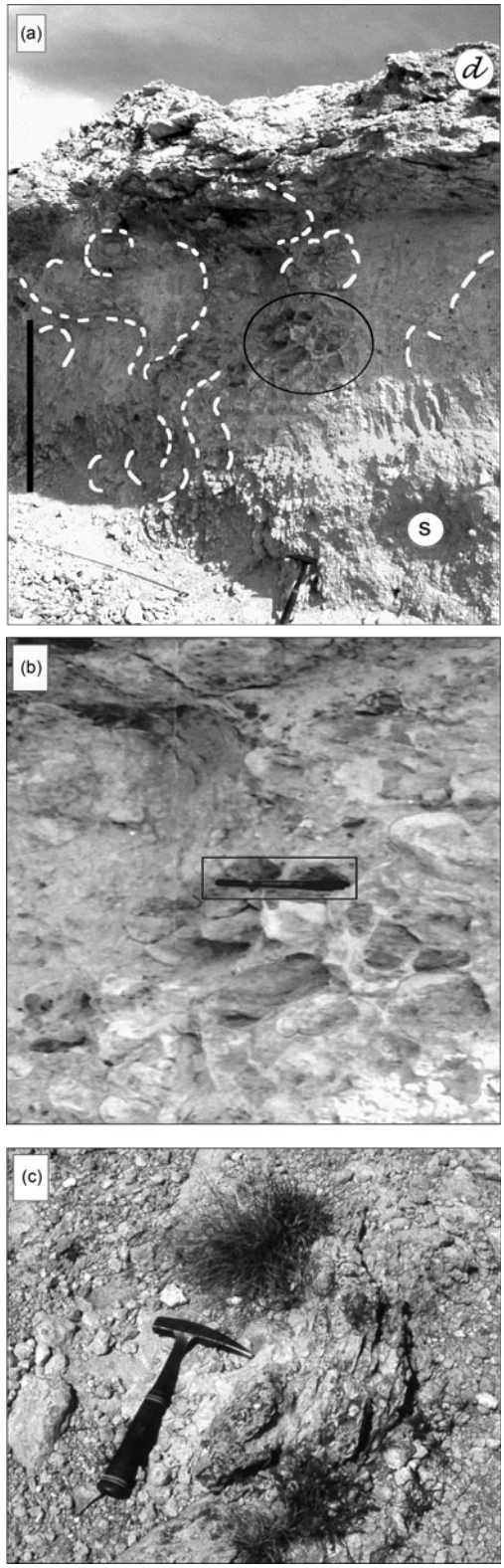

Figure 3. The highest level extends from ~36°50'–37°10' S to the north of the Valle de Chapalcó. (**a**) At the bottom of the exposure, the bedrock consists of siltites (s) and is covered by an accumulation of sandy silt with reworked clasts and silica concretions from the siltites. The small dark spots are basalt debris. The deposit is affected by involutions highlighted by white dashed lines. The duricrust (*d*) was also disturbed before hardening. The black bar = 1 m. The circle in the middle indicates the site of Figure 3b. (**b**) Detail of the central deformation with a septarian-like structure. The pencil (outlined by the white rectangle) = 14 cm. (**c**) A fold in the duricrust.

https://doi.org/10.1017/qua.2022.30 Published online by Cambridge University Press

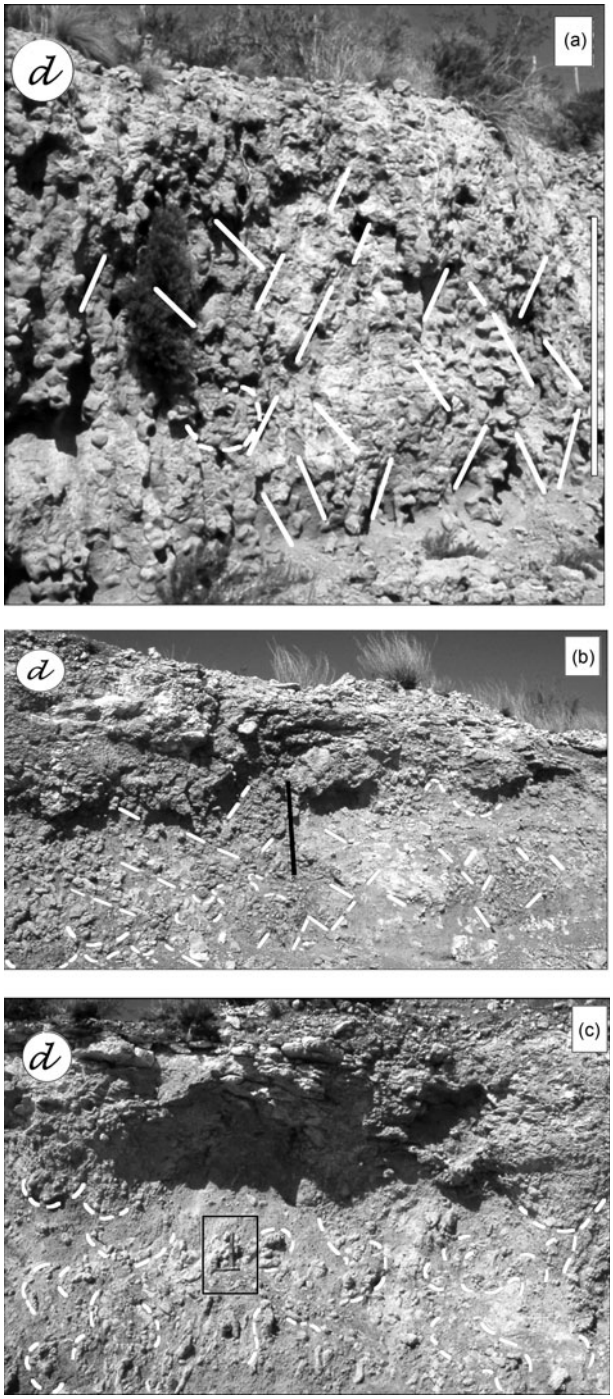

Figure 4. The intermediate level is present on the south-facing slope of the Valle de Hucal (64°23'–64°14'W, 37°78'–37°47'W; Fig. 1, site 2; Fig. 2, site 2; Fig. 4a–c). Several exposures, ~3 m high, are located along the longitudinal axis between provincial roads RP11 and RP9. *d* = duricrust. (**a**) An outcrop of siltites where the original layering has been destroyed by thermal contraction. The black lines show some contraction lineaments; scale bar to the right = 2 m. (**b**) Exposure of the stratigraphic units: at the bottom, siltites with whitish siliceous concretions; above is the alluvial cover consisting of silt, concretions, and gravel that has been greatly disturbed by thermal contraction; the deposit has lost its original stratification; clusters of pebbles appear in places; the coarse material is vertically arranged or follows the lineaments; the duricrust is disturbed, yet some portions maintain their original platy structure. Calcareous dust is mixed with alluvial material. The short white lines indicate some main lineaments. The bar = 1 m. (**c**) In the same valley, the disturbances are mostly involutions, indicated by white dashed lines. The hammer in the rectangle at the center gives the scale.

The Carapacha Chica exposure

The Carapacha Chica is an outcrop of Permian arkosic sandstone at the southwestern border of the Plateau in the Chadileuvú depression (~37°30'S, 66°10'W, 271 m above sea level; Fig. 1, site 3; Fig. 2, site 3; Fig. 5a, b). The rock is massive and very hard as a result of diagenesis and incipient metamorphic recrystallization. Thin sections show the absence of macro- and micro-porosity. At the foot of the north-facing slope at 260 m above sea level, an outcrop 3–3.5 m high and a few meters wide exposes from bottom to top: (1) ~150 cm of clasts with little sandy matrix; (2) ~30 cm of clasts slightly cemented with some matrix mixed with calcareous dust; (3) ~40 cm of clasts free of $CaCO_3$; (4) ~90 cm of clasts in a fine matrix mixed with calcareous dust; and (5) a duricrust ~40 cm thick. The bedrock is not visible. The material consists mostly of sand derived from fragmentation of the bedrock. The clasts are shattered rock debris, heterometric, no more than 10 cm across, with sharp edges. The original layering is rough, with the larger clasts parallel to the slope, poorly sorted. and not blunt, showing that they were not deposited by runoff. The layers have been deformed and involuted, suggesting creep structures.

A terrace of the Colorado River

On the terraces of the Colorado River, the alluvium consists of gravel with little sand and non-diastrophic structures most prominent at ~300 m above sea level. The sandy silt material is indurated, split along the layers, broken, and displaced into the overlying gravel. (Fig. 1, site 4; Fig. 2, site 4; Fig. 6a, b). There are no traces of faults in the terraces and the deformations are certainly not tectonic.

DISCUSSION

The initial impetus for this study was to discover whether there had been periglacial conditions immediately to the north of Patagonia where Pleistocene permafrost had been recognized. Several features observed in field exposures and under microscope have direct bearing on the answer to this question.

Hardening of the sediments

As observed in the cover deposits on the Plateau (Figs. 3, 4), the siltites are hardened and broken to decimeter-scale clasts. In the terraces of the Colorado River, the sand and silt beds are also indurated and split. Evaporation can desiccate surficial sand-silt beds, but not to the point of hardening them into solid rock. FitzPatrick (1956) and Pissart (1970) showed how frost strongly dehydrates fine-grained sediments, thereby modifying the structures and causing irreversible compaction. Freezing induces strong cryosmotic suction (negative pressure), which increases suction by 10 MPa for each 1°C decrease in temperature (Williams and Smith, 1989). In doing so, freezing extracts not only capillary and adsorbed water but also elements from minerals of the rocks and clasts.

Breakdown of rocks

The mechanism of freeze-thaw is generally invoked to explain mechanical weathering under temperate and cold climates. Freeze-thaw demands sufficient moisture, but here that was not the case considering the aridity in the region. In the exposure at the Carapaca Chica, the deposit consists entirely of detritus that cannot be ascribed to freeze-thaw processes on a rock lacking

https://doi.org/10.1017/qua.2022.30 Published online by Cambridge University Press

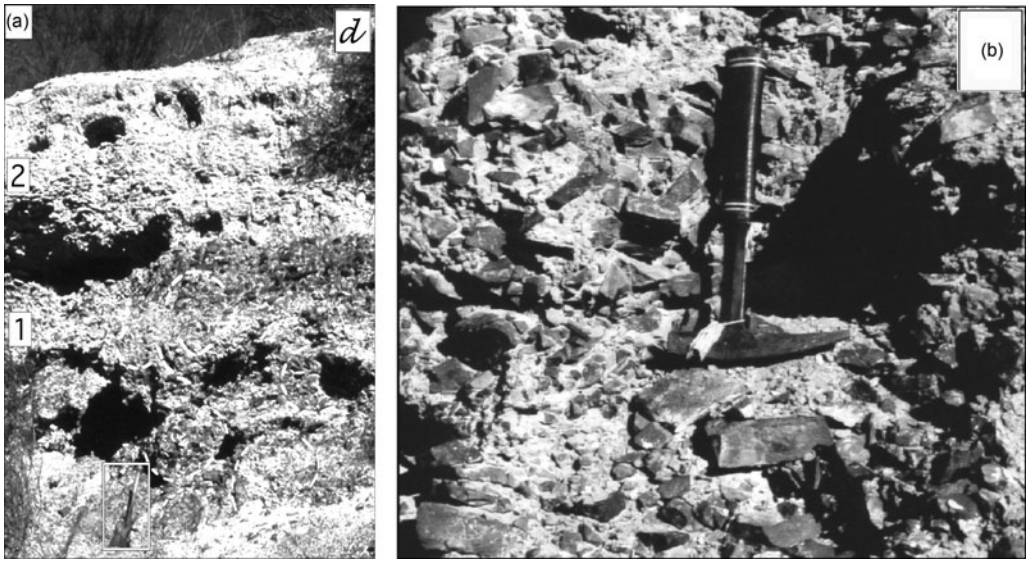

Figure 5. Carapacha Chica exposure (37°31.683′S, 66°24.550′W). (**a**) Shattered siliceous sandstone mixed with coarse sandy matrix in two distinct, slightly cemented layers (1 and 2); the white material is calcareous dust, secondarily spread over the whole exposure by rain and wind. The larger clasts are arranged parallel to slope. The white dashed lines indicate involutions, suggesting creep. The holes under the duricrust (*d*) are bird nests in the soft material. The spade in the rectangle at the bottom of the photograph indicates the scale. (**b**) In less-disturbed places, the larger clasts lay parallel to slope.

Figure 6. View of some stepped terraces of the Colorado River. The terraces of the Colorado River are present along the N-S Ruta 23 between 37°40'–38°S. In the southernmost and higher one, at ~300 m elevation, the disturbances are clearly visible. (**a**) In the foreground is the terrace at ~300 m above sea level. (**b**) an embankment ~1.5 m high exposes the deposit. The lower portion is mostly sand and boulders that have fallen from above. The fluvial sediment was heavily disturbed after cryo-suction and hardening.

https://doi.org/10.1017/qua.2022.30 Published online by Cambridge University Press

porosity. Thermal stress fatigue, as suggested by Hall (1999) in Antarctica, is a more likely explanation, especially at the latitude of La Pampa and on a north-facing slope. It should be born in mind that both the insolation and the daily thermal amplitude are greater than in Antarctica throughout the year, and therefore stress fatigue would be greater. Stress fatigue can happen only on bare rocks, however, and it takes a long time to produce significant amount of detritus; thus, the region must have been cold and dry for a long time.

Contraction and compression features

In both the uppermost (Valle de Chapalcó, Fig. 3a, b) and the intermediate (Valle de Hucal, Figs 4a–c) levels, the deposits have lost their original layering and are affected by cracks that cannot be ascribed to tectonic activity. There are no voids between the clasts and the enclosing material, as might be expected from desiccation: meter-scale desiccation cracks are only observed in muds and clays (vertisols). Differential thermal expansion and contraction, which can affect any type of solid material, is a more appropriate explanation, yet contraction of solid material needs low temperatures. Lachenbruch's (1962) explanation of rapid changes of temperature fits the observations. Strong insolation and, therefore, high daily thermal amplitude, both of which are typical in deserts, would have been the norm in La Pampa during the glaciations. Once formed, contraction cracks are permanent features and tend to propagate even deeper (Andersland and Al Moussawi, 1987; Williams and Smith, 1989).

Septaria, which occur in the uppermost level (Fig. 3a, b), arise from deformations caused by deep subaqueous burial loading under high fluid pressure, diagenesis, or seismic movements (Astin, 1986; Hounslow, 1997; Pratt, 2001; Seilacher, 2001; McMahon et al., 2017), yet none of these is appropriate here. Shrinkage, resulting from contraction and cryogenic compression, is most likely here.

Involutions

In the Valles de Chapalcó (Fig. 3a) and Hucal (Fig. 4c), as well as in the Carapacha Chica (Fig. 5a), the deposits are disturbed by involutions that could suggest solifluction. However, this slow mass movement demands a saturated material rich in colloidal elements and having a high water absorption capacity. This is not the case here because the $\leq$2 μm fraction represents <10% of the deposit mass.

As previously noted, the larger clasts in the Carapacha Chica lay parallel to slope, which excludes deposition by flows. In addition, the uphill catchment is too small to feed a flow that would have been strong enough to transport such a huge amount of detritus. The slope is also too gentle for debris to move downslope by gravity alone, and the sandy matrix mixed with calcareous dust would prevent plastic solifluction. Sliding on frost-hardened ground and gelifluction (solifluction on frozen ground) are more likely processes. Frozen ground prevents infiltration, favoring saturation of the overlying layer and, consequently, fluidal episodes after snow or rainfall.

Significance of the calcareous dust

Calcareous dust closely associated with Pleistocene periglacial deposits occurs in Argentina from southern Patagonia to the Mendoza Pre-Cordillera at 33°S and perhaps even farther north. The $CaCO_3$ carbonate is calcite, which appears under the SEM as loose idiomorphic rhombohedral and scalenohedral crystals, predominantly of micrite (<5 μm across). Techer et al. (2014) and Vogt et al. (2018) showed from analyses of the strontium, carbon, and oxygen isotope compositions, and of the rare-earth element distributions, that this calcite is not of marine origin but continental—not pedogenic but glaciogenic. The carbonate was transported in glacial meltwater and deposited on the emerged continental shelf where it crystallized. From there it was picked up, carried, and widely dispersed by southeasterly winds.

This dust therefore indicates glacial episodes; in this region the dust occurs in sediments that were deposited during the Pleistocene. The preservation of a fragile, powdery and easily dissolved calcite for such a long time means that there was no tundra cover with acidic (pH ~3.5) water percolation, and therefore aridity persisted during the entire Pleistocene and Holocene. In continental Antarctica, mid-Miocene cooling caused extinction of the tundra (Adam et al., 2008), which suggests that the climate was cold and arid enough in the region to prevent the growth of a vegetation cover.

The cold arid environment

As noted above, this part of Argentina was a cold desert during most of the Pleistocene. In cold deserts, as was the case here, little ice forms. Cameron (1971), Van Everdingen (1976), Bockheim and Tarnocai (1998), and Bockheim and McLeod (2006) stated that the moisture (ice) content of the driest Antarctic soils approaches that of the driest desert soils in cold and hot deserts ($\leq$5% by volume). One cannot expect conspicuous features due to ice segregation and upheaval of the ground. With such limited moisture availability, frost action is restricted to thermal contraction, in addition to stresses and related disturbances that produce features not obvious enough to discriminate between seasonally or perpetually frozen ground. Difficulty in separating the effects from seasonal and perpetual frozen ground is documented in other regions, such as in hypercontinental southeastern Siberia where both past and present permafrost are well established, and yet rock shattering and gelifluction remain dominant (Vogt and Larqué, 2002).

The exposures examined here contain split rocks, which are features of thermal contraction in coarse material, and deposits produced by gelifluction and creep. All are characteristic of cold conditions, although not necessarily cold enough for the ground to be permanently frozen. Yet, as Chen et al. (1993) showed experimentally, powdered calcium carbonate reduces the frost-susceptibility of sediments and, therefore, lower temperatures are needed for cryogenic features to form. It follows that the cryogenic features observed in La Pampa testify for very cold conditions. According to González and Corte (1976), the temperature fell at González Chavez (38°S) by approximately 20°C, with mean annual temperatures of −5 to −6° or less in contrast to the current 14.5°C. This suggests that the average annual temperature in La Pampa was <0°C.

Organic matter is almost completely absent in Antarctic gelisols (Beyer et al., 1999), and the biological component of the soil is nil in most situations (Campbell and Claridge, 1981, 2009). Altogether, the facts observed in the study region point to a landscape of long-lasting bare ground devoid of vegetation, with only calcified fungal hyphae and spores found with the calcareous dust.

https://doi.org/10.1017/qua.2022.30 Published online by Cambridge University Press

Microscopic observations

Microscopic analysis showed lamellar crystals of calcite and gypsum and clay minerals changed into opal. Such features are observed only in cold regions where permafrost currently exists, such as in Antarctica, and in regions where permafrost formed during glacial episodes, as in Patagonia, the Mendoza Precordillera, Canada, France, and southeastern Siberia (Vogt, 1990; Vogt and Corte, 1996; Vogt and Larqué, 1998, 2002).

The presence of calcite and gypsum

Hallet (1976) conducted freezing experiments of carbonate-rich water at initial Ca concentrations of $0.77–3.8 \times 10^{-4}$ M, with a final concentration of Ca^{2+} as much as 50 times that of the initial parent solution. Such increased concentrations depress the freezing point significantly below 0°C. Once this point is reached, supersaturated solutions precipitate with instantaneous freezing. If several solutes are present, a sequence of minerals precipitates as the solution becomes successively supersaturated for each one. Formation of these precipitates requires very low temperatures (Hallet, 1979), together with time and stable thermal conditions of still water in a closed system. The preferential sites for such changes are residual lenses filled with liquid water in permafrost. In an unfrozen sediment, or in active layers that behave as open systems, many thermal, mechanical, and hydrologic changes take place and mobile pore fluids can circulate. This allows vegetation to grow and organic acids, which would dissolve the calcite, to form.

The new crystals have a lamellar habit and tend to pile up. In some deposits of La Pampa, lamellar calcite crystals form coatings and fringes between the clasts. This means that the primary calcite dissolved and re-crystallized when the solution became supersaturated. Lamellar crystals of gypsum, identical to those observed here, can be seen now in Antarctica. Such crystals have been reported only in permafrost environments (Vogt and Corte, 1996; Fig. 7a–c).

The transformation of clay to opal

Vogt and Larqué (1998, 2002) described the transformation of clay material into opal in Patagonian Pleistocene deposits that had been affected by permafrost. Roy et al. (1995) emphasized that high suctions that develop near the freezing front can change the structure of clay minerals that occur in the sediment. Suction increases with decreasing temperature, as happens in lenses filled with residual fluids within the permafrost. The confined supersaturated solutions can last long enough to cause chemical transformations and breakdown of the crystals because the freezing point will only be reached at very low temperatures. Once their structure is destroyed, the clay minerals lose cations, except silicon, and change into opal. This neoformation of opal is observed widely in the Pleistocene sediments of La Pampa. SEM observations show the transition of clay aggregates and coatings into opal (Fig. 8). Transformation of clay into opal in the natural world seems restricted to permafrost conditions.

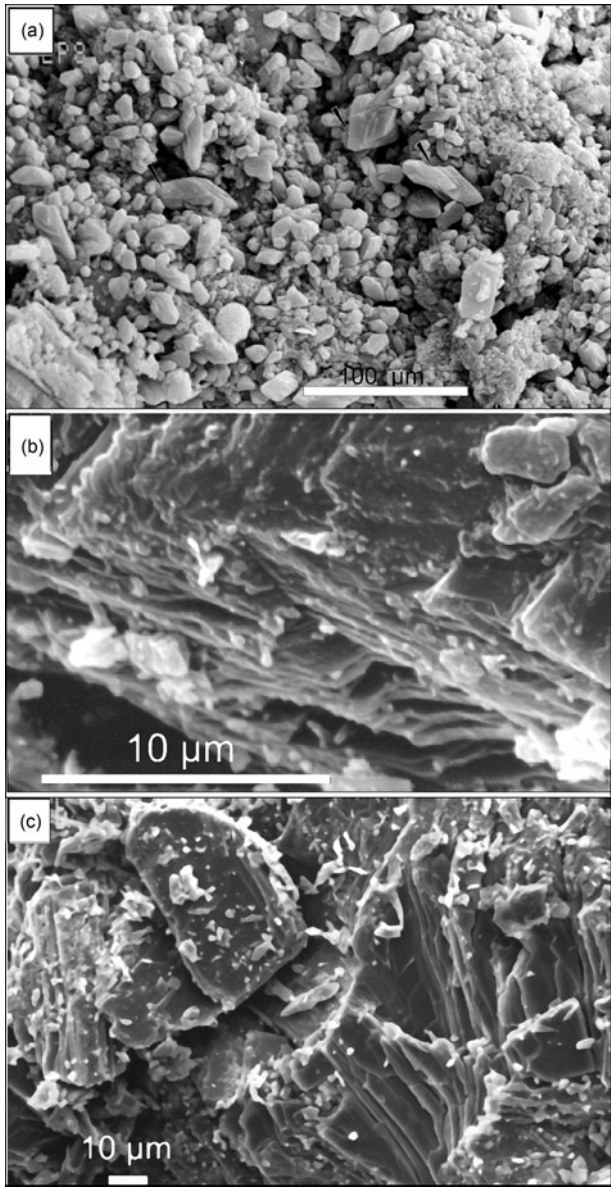

Figure 7. SEM images of sediments from the La Pampa exposures. (**a**) Loose rhomboidal and scalenohedral calcite particles; (**b**) lamellar calcite crystals typical of a precipitation by freezing; (**c**) lamellar structure of gypsum.

CONCLUSIONS

Pleistocene ice wedges in the lowlands of Argentina near Puerto Madryn (42°48'S) are impressive in size, reaching 3 m depth. They were ascribed to the LGM on the basis of ^{14}C data. Similar structures occur all along the littoral Ruta Nacional 3 (RN3) road as far as the Colorado River. It is known from other evidence that the Polar Front had shifted to 51°S and perhaps even as far north as 45°S. Evidently, sub-zero annual temperatures must have existed during the Pleistocene period between 39–36°S.

From a geomorphological point of view, knowledge of the events that happened during the Pleistocene glaciations in this region is still poor, therefore more investigations on the Andean piedmont uphill and in the plains would be welcomed. Periglacial features in the La Pampa region are much less conspicuous than those in the nearby Patagonia, making it difficult to recognize them. The climate was somewhat warmer and the glaciers and ice caps were much farther away. There are no paleontological remains in the Pleistocene deposits, which suggests that the environment was very dry, probably with very little ice. Microscopic alterations to the minerals and changes in the chemistry are characteristic of permafrost.

https://doi.org/10.1017/qua.2022.30 Published online by Cambridge University Press

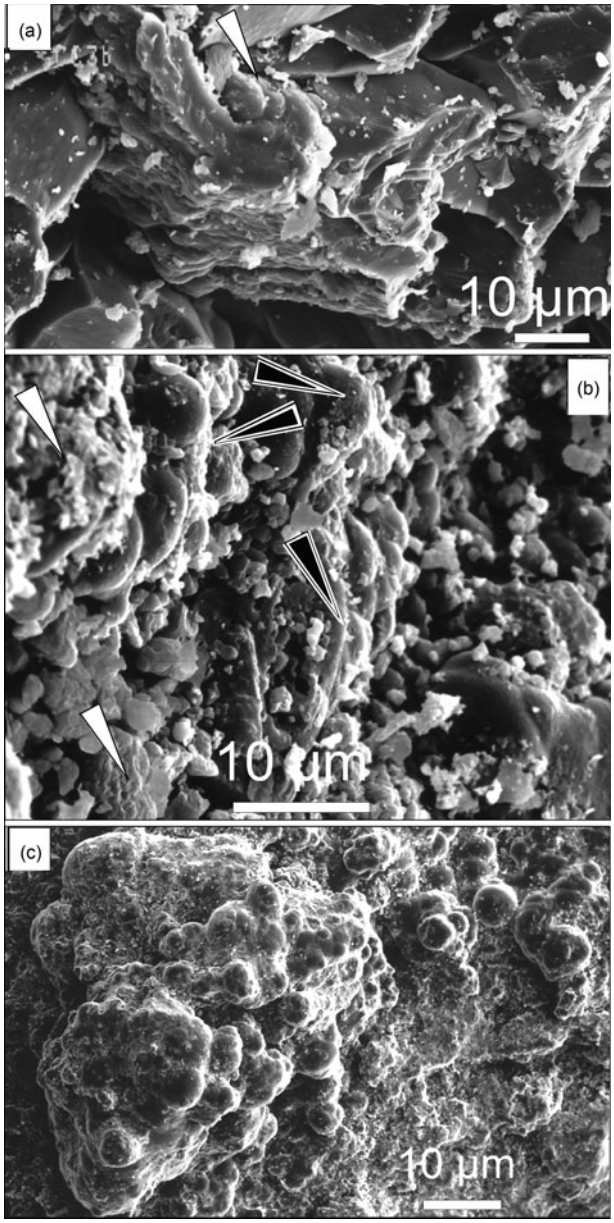

Figure 8. SEM images of sediments of La Pampa exposures. (**a**) Mica particle with opal growing above (white arrow); (**b**) the white arrow at the left bottom indicates a mica particle; the white arrow at the top left indicates disordered clay particles; the black arrows indicate the intimate contact between clay and opal; (**c**) opal concretions as a final result.

Nonetheless, enough evidence has been found to indicate that the temperature decreased enough during the glacial episodes to produce permafrost in the lowlands of Argentina between 40–36°S latitude. This finding moves the limits of permafrost ~200 km farther north than has been recognized previously.

Acknowledgments. Field work was done with my husband H. Vogt, who has died since. J. Dorth and D. Booth, Editors, and the two reviewers are sincerely thanked for their constructive comments. N. Clauer of the ISTES from Strasbourg University followed the work progress step by step while bringing suggestions and improvements. Last but not least, R. Webster from Rutheford Experimental Station transformed a groping draft into clear English language and added interesting remarks. This work was supported by a teaching and research agreement between the Universities of Strasbourg and La Pampa.

REFERENCES

Adam, R., Lewis, A.R., Marchant, D.R., Ashworth, A.C., Hedenäs, L., Hemming, S.R., Johnson, J.V., *et al.*, 2008. Mid-Miocene cooling and the extinction of tundra in continental Antarctica. *PNAS* **105**, 10676–10680.

Andersland, O.B., Al-Moussawi, H.M., 1987. Crack formation in soil landfill covers due to thermal contraction. *Waste Management & Research* **5**, 445–452.

Annan, J.D., Hargreaves, J.C., 2013. A new global reconstruction of temperature changes at the last glacial maximum. *Climate of the Past* **9**, 367–376.

Astin, T.R., 1986. Septarian crack formation in carbonate concretions from shales and mudstones. *Clay Minerals* **21**, 617–631.

Aumassanne, C.M., Gaspari, F.J., Bege, M.E., Sartor, P.D., Oricchio, P., Di Bella, C.M., 2018. Morfometría de la cuenca alta del río Colorado, Argentina. *Boletín Geográfico* **40**, 13–29.

Barker, P.F., 2007. The history of Antarctic Peninsula glaciation. In: Cooper A.K., Raymond C.R., ISAES Editorial Team. (Eds), *Antarctica: A Keystone in a Changing World*. Online Proceedings of the 10th ISAES), USGS Open-File Report 1047, Short Research Paper 042, 5 pp. https://doi.org/10.3133/ofr20071047SRP042.

Barron, J., Larsen, B., Baldauf, J.G., 1991. Evidence for late Eocene to early Oligocene Antarctic glaciation and observations on Neogene glacial history in Antarctica; Results from Leg 119. *Proceedings of the Ocean Drilling Program, Scientific Results* **119**, 869–891.

Bart, P.J., Egan, D., Warny, S.A., 2005. Direct constraints on Antarctic Peninsula ice sheet grounding events between 5.12 and 7.94 Ma. *Journal of Geophysical Research* **110**, F04008. https://doi.org/10.1029/2004JF000254.

Becquey, S., Gersonde, R., 2002. Past hydrographic and climatic changes in the Subantarctic Zone of the South Atlantic—the Pleistocene record from ODP Site 1090. *Palaeogeography, Palaeoclimatology, Palaeoecology* **182**, 221–239: doi.org/10.1016/S0031-0182(01)00497-7.

Benn, D.I., Clapperton, C.M., 2000. Glacial sediment-landform associations and paleoclimate during the last glaciation, Strait of Magellan, Chile. *Quaternary Research* **54**, 513–523.

Bernardi, M.I., Bertotto, G.W., Orihashi, Y., Sumino, H., Ponce, A.D., 2019. Volcanology and geochronology of very long Neogene–Quaternary basaltic flows from southeast Payenia, central-west Argentina. *Andean Geology* **46**, 490–525. dx.doi.org/10.5027/andgeov46n3-3181.

Beyer, L., Bockheim, J.G., Campbell, I.B., Claridge, G.G.C., 1999. Genesis, properties and sensitivity of Antarctic Gelisols. *Antarctic Science* **11**, 387–398.

Blisniuk, P.M., Stern, L.A., Chamberlain, C.P., Idleman, B., Zeitler, P.K., 2005. Climatic and ecologic changes during Miocene surface uplift in the southern Patagonian Andes. *Earth and Planetary Science Letters* **230**, 125–142: doi.org/10.1016/j.epsl.2004.11.015.

Bockheim, J.G., McLeod, M., 2006. Soil formation in Wright Valley, Antarctica since the late Neogene. *Geoderma* **137**, 109–116: doi:10.1016/j.geoderma.2006.08.028.

Bockheim, J.G., Tarnocai, C., 1998. Nature, occurrence and origin of dry permafrost. In: Lewkowicz, A.G., Allard, M. (Eds), *Proceedings of the 7th International Conference on Permafrost. Collection Nordicane (Université Laval)* **57**, 57–63.

Buschiazzo, D.E., Martinez, H.M., Peinemann, N., 1987. Condiciones Paleoclimáticas Deducidas de Indicatores Pedológicos y Geomorfológicos en la Región Pampeana Central (Argentina). *Zentralblatt Geologie Paläontologie* **1**, 875–883.

Calmels, A.P., Casadío, S., 2004. *Compilación Geológica de la Provincia de La Pampa*. Amerindia, Santa Rosa.

Calmels, A.P., Visconti, G., Carballo, O.C., Sbrocco, J.A., 1996. *Los sedimentos del Pleistoceno tardio–Holoceno encauzados en el Valle de Quehué, Provincia de La Pampa*. Actas VI Reunión Argentina Sedimentología, Bahia Blanca, Argentina, pp. 135–140.

Cameron, R.E., 1971. Antarctic soil microbial and ecological investigations. In: Quam, L.O., Porter, H.D. (Eds.), *Research in the Antarctic*. American Association for the Advancement of Science, Washington, D.C., pp. 137–189.

Campbell, I.B., Claridge, G.G.C., 1981. Soil research in the Ross Sea region of Antarctica. *Journal of the Royal Society of New Zealand* **11**, 401–410.

Campbell, I.B., Claridge, G.G.C., 2009. Antarctic permafrost soils. In: Margesin, R. (Ed.), *Permafrost Soils*. Springer, Berlin, pp. 17–31: DOI: 10.1007/978-3-540-69371-0.

https://doi.org/10.1017/qua.2022.30 Published online by Cambridge University Press

Casadío, S., Schulz, A., 1986. Sobre los sedimentos lacustres (Formación Santa Rosa) del Pleistoceno superior, La Pampa, Argentina. *Universidad Nacional de La Pampa. Series Supplement* **3**, 169–176. Santa Rosa, Provincia de La Pampa. .

Cavallotto, J.L., Violante, R.A, Hernández-Molina, F.J., 2011. Geological aspects and evolution of the Patagonian continental margin. *Biological Journal of the Linnean Society* **103**, 346–362: doi.org/10.1111/j.1095-8312.2011.01683.x.

Caviedes, C.N., Paskoff, R., 1975. Quaternary glaciations in the Andes of north-central Chile. *Journal of Glaciology* **14**, 155–170.

Chen, X., Corte, A.E., Wang, Y., Shen, Y., 1993. Frost susceptibility of powdered calcium carbonate. *6th International Conference Proceedings on Permafrost, Beijing, China, July 5–9, 1993*. South China University of Technology Press, Wushan Guangzhou (China), v. 2, pp. 1073–1075.

Chow, J.M., Bart, P.J., 2003. West Antarctic Ice Sheet grounding events on the Ross Sea outer continental shelf during the Middle Miocene. *Palaeogeography, Palaeoclimatology, Palaeoecology* **198**, 169–186: doi.org/10.1016/S0031- 0182(03)00400-0.

Christeleit, E.C., Brandon, M.T., Shuster, D.L., 2017. Miocene development of alpine glacial relief in the Patagonian Andes, as revealed by low-temperature thermochronometry. *Earth and Planetary Science Letters* **460**, 152–163: doi.org/10.1016/j.epsl.2016.12.019.

Clapperton, C.M., 1993. *Quaternary Geology and Geomorphology of South America*. Elsevier, Amsterdam.

Clapperton, C.M., 1994. The Quaternary glaciation of Chile: a review. *Revista Chilena de Historia Natural* **67**, 369–383.

Colwyn, A.D., Brandon, M.T., Hren, M.T., Hourigan, J., Pacini, A., Cosgrove, M.G., Midzik, M., Garreaud, R.D., Metzger C., 2019. Growth and steady state of the Patagonian Andes. *American Journal of Science* **319**, 431–472: doi.org/10.2475/06.2019.01].

Coronato, A., Martínez, O., Rabassa, J., 2004. Glaciations in Argentine Patagonia, southern South America. In: Ehlers, J., Gibbard, P.L. (Eds), *Quaternary Glaciations—Extent and Chronology, Part III*. Elsevier, Amsterdam, pp. 49–67.

Corte, A.E., 1967. Informe preliminar del progreso efectuado en el estudio de las estructuras de crioturbación Pleistocenas fósiles en la provincia de Santa Cruz. *Terceras Jornadas Geológicas Argentinas* **2**, 9–17.

Corte, A.E., 1983. Procesos periglaciales actuales y pasados (Pleistocénicos) en Argentina Central. *Acta Geocriogénica* (*Mendoza*) **1**, 62–74.

Corte, A.E., 1991. Chronostratigraphic correlations of cryogenic and glacigenic episodes in Central Andes with Patagonia. *Permafrost and Periglacial Processes* **2**, 67–70: doi.org/10.1002/ppp.3430020111.

Corte, A.E., Beltramone, C., 1984. Edad de la estructuras geocryogénicas de Puerto Madryn (Chubut). *Acta Geocriogénica* (*Mendoza*) **2**, 66–72.

Cortese, G., Gersonde, R., Hillenbrand, C.-D., Kuhn, G., 2004. Opal sedimentation shifts in the world ocean over the last 15 Myr. *Earth and Planetary Science Letters* **224**, 509–527: doi.org/10.1016/j.epsl.2004.05.035.

Crosta, X., 2009. Antarctic sea ice history, late Quaternary. In: Gornitz, V. (Ed.), *Encyclopedia of Paleoclimatology and Ancient Environments*. Springer, Berlin, pp. 21–23.

Crosta, X., Pichon, J.-J., Burckle, L.H., 1998. Application of modern analog technique to marine Antarctic diatoms: reconstruction of maximum sea-ice extent at the last glacial maximum. *Paleoceanography* **13**, 284–297: doi.org/10.1029/98PA00339.

Czajka, W., 1955. Rezente und Pleistozäne Verbreitung und Typen des periglazialen Denudationszyklus in Argentinien. *Acta Geographica* **14**, 121–140.

Dingle, R.V., Lavelle, M., 2017. Antarctic Peninsular cryosphere: early Oligocene (c. 30 Ma) initiation and a revised glacial chronology. *Journal of the Geological Society* **155**, 433–437. doi.org/10.1144/gsjgs.155.3.0433.

Elliott, C., 2006. *Physical Rock Weathering along the Victoria Land Coast, Antarctica*. Ph.D. thesis, University of Canterbury, Christchurch, New Zealand, 289 pp.

FitzPatrick, E.A., 1956. An indurated soil horizon formed by permafrost. *Journal of Soil Science* **7**, 248–254.

Flohn, H., 1988. *Das Problem der Klimaänderungen in Vergangenheit und Zukunft*. Wissenschaftliche Buchgesellschaft, Darmstadt.

Flower, B.P., Kennett, J., 1994. The Middle Miocene climatic transition: East Antarctic ice sheet development, deep ocean circulation and global carbon cycling. *Palaeogeography, Palaeoclimatology, Palaeoecology* **108**, 537–555: doi.org/10.1016/0031-0182(94)90251-8.

Folguera, A., Zárate, M.A., 2009. La sedimentación Neógena continental en el sector extrandino de Argentina Central. *Revista de la Asociación Geológica Argentina* **64**, 692–712.

Francis, J.E., Marenssi, S., Levy, R., Hambrey, M., Thorn, V.T., Mohr, B., Brinkhuis, H., *et al.*, 2009. From greenhouse to icehouse—the Eocene/Oligocene in Antarctica. In: Florindo, F., Siegert, M. (Eds.), *Developments in Earth & Environmental Sciences*. Elsevier, The Netherlands, v. **8**, pp. 311–372.

García, J.L., Kaplan, M., Hall, B.L., Schaefer, J.M., Vega, R., Schwartz, R., Finke, R.C., 2012. Glacier expansion in southern Patagonia throughout the Antarctic Cold Reversal. *Geology* **40**, 859–862: doi.org/10.1130/G33164.1.

Ghiglione, M.C., Ramos, V.A., Cuitiño, J., Barberón, V., 2016. Growth of the Southern Patagonian Andes (46–53°S) and their relation to subduction processes. In: Folguera, A., Naipauer, M., Sagripanti, L., Ghiglione, M.C., Orts, D.L., Giambiagi, L. (Eds.), *Growth of the Southern Andes*. Springer Earth System Sciences, Springer, Cham, Switzerland, pp. 201–240.

Giai, S.B., Tullio, J.O., 1998. Características de los principales acuiferos de la Provincia de La Pampa. *Revista Geología Aplicada a la Ingenieria y al Ambiente* **12**, 51–68.

Glasser, N.F., Jansson, K.N., 2008. The glacial map of southern South America. *Journal of Maps* **4**, 175–196: doi.org/10.4113/jom.2008.1020.

González, M.A., Corte, A.E., 1976. Pleistocene geocryogenic structures at 38° S.L., 60° LW, and 200 m above sea level, González Chávez, Buenos Aires Province, Argentina. *Biuletyn Peryglacjalny* **25**, 23–33.

Griffing, C.Y., Barendragt, R.W., Clague, J.J., Roberts, N.J., Corbella, H., Ercolano, B., Rabassa, J., 2012. Magnetostratigraphy of continental glacial deposits in southernmost Patagonia. *AGU* 2012 *Fall Meeting, San Francisco, CA, Abstract GP*13*B*-1120.

Guilderson, T., Burckle, L., Hemming, S., Peltier, W.R., 2000. Late Pleistocene sea level variations derived from the Argentine Shelf. *Geochemistry Geophysics Geosystems* **1**. https://doi.org/10.1029/2000GC000098.

Gutiérrez, M.A., Escostegui, L., Espejo, P., 2019. *Hoja Geológica 3766-II Victorica. Programa Nacional de Cartas Geológicas de la República Argentina*. Servicio Geológico Minero Argentino (SEGEMAR). Instituto de Geología y Recursos Minerales Boletín 437, 64 pp.

Hall, K., 1999. The role of thermal stress fatigue in the breakdown of rock in cold regions. *Geomorphology* **31**, 47–73: doi.org/10.1016/S0169- 555X(99)00072-0.

Hallet, B., 1976. Deposits formed by subglacial precipitation. *Geological Society of America Bulletin* **87**, 1003–1015.

Hallet, B., 1979. Solute redistribution in freezing ground. In: National Research Council Canada, *Proceedings 3rd International Conference on Permafrost, July 10–13, 1978, Edmonton, Alberta*. National Research Council, Ottawa, pp. 86–91.

Haywood, A.M., Smellie, J.L., Ashworth, A.C., Cantrill, D.J., Florindo, F., Hambrey, M.J., Hill, D., *et al.*, 2009. Middle Miocene to Pliocene history of Antarctica and the Southern Ocean. In: Florindo, F., Siegert, M. (Eds.), *Developments in Earth & Environmental Sciences*. Elsevier, The Netherlands, v. 8, pp. 401–463.

Holbourn, A., Kuhnt, W., Frank, M., Haley, B.A., 2013. Changes in Pacific Ocean circulation following the Miocene onset of permanent Antarctic ice cover. *Earth and Planetary Science Letters* **365**, 38–50: doi.org/10.1016/j.epsl.2013.01.020.

Hounslow, M.W., 1997. Significance of localized pore pressures to the genesis of septarian concretions. *Sedimentology* **44**, 1133–1147.

Hulton N.R.J., Purves R.S., McCulloch R.D., Sugden D.E., Bentley M.J., 2002. The last glacial maximum and deglaciation in southern South America. *Quaternary Science Reviews* **21**, 233–241: doi.org/10.1016/S0277- 3791(01)00103-2.

Ingólfsson, Ó., 2004. The Quaternary glacial and climate history of Antarctica. In: Ehlers, J., Gibbard, P.L. (Eds.), *Quaternary Glaciations of the World, Part III*. Kluwer, Dordrecht, pp. 3–43.

Iriondo, M.H., Kröhling, D.M., 1995. El sistema eólico pampeano. *Comunicaciones Museo Provincial Ciencias Naturales "Florentino Ameghino"* (*n.s.*), *Santa Fé* **5**, 1–45.

Isla, F.I., Espinosa, M. A., 1995. Coastal environmental changes associated with Holocene sea level fluctuation: southeastern Buenos Aires, Argentina. *Quaternary International* **26**, 55–60: doi.org/10.1016/1040-6182(94)00046-8.

https://doi.org/10.1017/qua.2022.30 Published online by Cambridge University Press

Ivany, L.C., Van Simaeys, S., Domack, E.W., Samson, S.D., 2005. Evidence for an earliest Oligocene ice sheet on the Antarctic Peninsula. *Geological Society of America Bulletin* **34**, 377–380: doi.org/10.1130/G22383.1.

Kaiser, J., Lamy, F., Hebbeln, D., 2005. A 70-kyr sea surface temperature record off southern Chile (Ocean Drilling Program Site 1233). *Paleoceanography* **20**, PA4009. https://doi.org/10.1029/2005PA001146.

Katz, M.E., Miller, K.G., Wright, J.D., Wade, B.S., Browning, J.V., Cramer, B.S., Rosenthal, Y., 2008. Stepwise transition from the Eocene greenhouse to the Oligocene icehouse. *Nature Geoscience* **1**, 329–334: doi:10.1038/ngeo179.

Kay, S.M., Burns, W.M., Copeland, P., Mancila, O., 2006. Upper Cretaceous to Holocene magmatism evidence for transient Miocene shallowing of the Andean subduction zone under the northern Neuquén Basin. In: Kay, S.M., Ramos, V.A. (Eds.) *Evolution of an Andean Margin: a Tectonic and Magmatic View from the Andes to the Neuquén Basin (35°–39°S Lat)*. Geological Society of America, Special Paper 407, 19–60.

Kohfeld, K.E., Harrison, S.P., 2001. DIRTMAP: the geological record of dust. *Earth Science Reviews* **34**, 81–114: doi.org/10.1016/S0012-8252 (01)00042-3.

Konishchev, V.N., 1982. Characteristics of cryogenic weathering in the permafrost zone of the European USSR. *Arctic and Alpine Research* **14**, 261–265.

Lachenbruch, A.H., 1962. Mechanics of thermal contraction cracks and ice-wedge polygons in permafrost. *Geological Society of America Special Paper* **70**, 1–69.

Le Roux, J.P., 2012a. A review of Tertiary climate changes in southern South America and the Antarctic Peninsula. Part 1: oceanic conditions. *Sedimentary Geology* 247–248, 1–20: doi.org/10.1016/j.sedgeo.2011.12.014.

Le Roux, J.P., 2012b. A review of Tertiary climate changes in southern South America and the Antarctic Peninsula. Part 2: continental conditions. *Sedimentary Geology* 247–248, 21–38: doi.org/10.1016/j.sedgeo.2011. 12.001.

Levitan, M.A., Leichenkov, G.L., 2014. Cenozoic glaciation of Antarctica and sedimentation in the Southern Ocean. *Lithology and Mineral Resources* **49**, 117–113: doi.org/10.1134/S0024490214020060. .

Linares, E., Llambías, E.J., Latorre, C.O., 1980. Geología de la Provincia de La Pampa, República Argentina y geocronología de sus rocas metamórficas y eruptivas. *Revista Asociación Geológica Argentina* **35**, 87–146.

Liss, C.-Ch., 1969. Fossile Eiskeile (?) an der Patagonischen Atlantikkuste. *Zeitschrift für Geomorphologie* **13**, 109–114.

Lliboutry, L., 1956. *Nieves y Glaciares de Chile. Fundamentos de Glaciologia*. Universidad de Chile, Santiago de Chile, 471 pp.

López-Martínez, J., Serrano, E., 2005. Permafrost and periglacial processes in Hurd Peninsula, Livingston Island, Maritime Antarctica. *2nd European Conference on Permafrost : EUCOP II, June 12–16, 2005, Potsdam, Germany: Programme and Abstracts*. Alfred-Wegener-Stiftung, Berlin, p. 75.

López-Martínez, J., Schmid, T., Serrano, E., Mink, S., Nieto A., Guillaso, S., 2016. Geomorphology and surface landforms distribution in selected ice-free areas in the South Shetland Islands, northern Antarctic Peninsula region. *Cuadernos de Investigación Geográfica* **42**, 435–455.

Lorenz, W., 2002. The "Calcreta Principal" ("tosca") at the border of the provinces of La Pampa and Buenos Aires. *Zeitschrift Angewandte Geologie* **1**, 44–51.

MARGO Project Members, 2009. Constraints on the magnitude and patterns of ocean cooling at the last glacial maximum. *Nature Geoscience* **2**, 127–132: doi.org/10.1038/NGEO411.

McClymont, E.L., Elmore, A.C., Kender, S., Leng, M.J., Greaves, M., Elderfield, H., 2016. Pliocene–Pleistocene evolution of sea surface and intermediate water temperatures from the southwest Pacific. *Paleoceanography* **31**, 895–913: doi:10.1002/2016PA002954.

McMahon, S., van Smeerdijk Hood, A., Mcilroy, D., 2017. The origin and occurrence of subaqueous sedimentary cracks. In: Brasier, A.T., McIlroy, D., McLoughlin, N. (Eds.), Earth System Evolution and Early Life: A Celebration of the Work of Martin Brasier. *Geological Society, London, Special Publications* **448**, 285–309.

Mehl, A.E., Zárate, M.A., 2007. Litologia y genesis de los depositos del Cenozoico tardio del Bajo del Durazno, Provincia de La Pampa, Argentina. *Latin American Journal of Sedimentology and Basin Analysis* **14**, 129–142.

Melchor, R.N., Casadío, S.A., 1999. Descripción de la Hoja Geológica 3766-III "La Reforma" (1:250.000), Provincia de La Pampa. Instituto de Geología y Recursos Minerales. *Boletín Servicio Geológico Minero Argentino* **295**, 1–56.

Mercer, J.H., Sutter, F., 1982. Late Miocene–Earliest Pliocene glaciation in Southern Argentina. Implications for global ice-sheet history. *Palaeogeography, Palaeoclimatology, Palaeoecology* **38**, 185–206.

Moeller, P., Hjort, C., Björck, S., Rabassa, J., Ponce, J., 2010. Late Quaternary glaciation history of Isla de los Estados, southeasternmost South America. *Quaternary Research* **73**, 521–534: doi.org/10.1016/ j.yqres.2010.02.004.

Ochsenius, C., 1985. Pleniglacial desertization, large-animal mass extinction and Pleistocene-Holocene boundary in South America. *Revista de Geografía Norte Grande* **12**, 35–47.

Paskoff, R., 1967. Los cambios climáticos Plio-Cuaternarios en la franja costera de Chile semi-árido. *Boletin Asociación de Geógrafos de Chile* **1**, 11–13.

Passchier, S., Browne, G., Field, B., Fielding, C.R., Krissek, L.A., Panter, K., Pekar, S.F., ANDRILL-SMS Science Team, 2011. Early and Middle Miocene Antarctic glacial history from the sedimentary facies distribution in the AND-2A drill hole, Ross Sea, Antarctica. *Geological Society of America Bulletin* **123**, 2352–2365: doi.org/10.1130/B30334.1.

Pissart, A., 1970. Les phénomènes physiques essentiels liés au gel, les structures périglaciaires qui en résultent et leur signification climatique. *Annales Société Géologique Belgique* **93**, 7–49.

Pratt, B.R., 2001. Septarian concretions: internal cracking caused by synsedimentary earthquakes. *Sedimentology* **48**, 189–213.

Rabassa, J., 2008. Late Cenozoic glaciations in Patagonia and Tierra del Fuego. In: Rabassa, J. (Ed.), The Late Cenozoic of Patagonia and Tierra del Fuego. *Developments in Quaternary Sciences* **11**, 151–204.

Rabassa, J., Coronato, A., Salemme, M., 2005. Chronology of the Late Cenozoic Patagonian glaciations and their correlation with biostratigraphic units of the Pampean region (Argentina). *Journal of South American Earth Sciences* **20**, 81–103: doi.org/10.1016/j.jsames.2005.07.004.

Rabassa, J., Coronato, A., Martinez, O., 2011. Late Cenozoic glaciations in Patagonia and Tierra del Fuego: an updated review. *Biological Journal of the Linnean Society* **103**, 316–335: doi.org/10.1111/j.1095- 8312.2011.01681.x.

Ramos, V.A., Ghiglione, M.C., 2008. Tectonic evolution of Patagonian Andes. In: Rabassa J. (Ed.), The Late Cenozoic of Patagonia and Tierra del Fuego. *Developments in Quaternary Sciences* **11**, 57–71.

Rech, J.A., Currie, B.S, Shullenberger, E.D., Dunagan, S.P., Jordan, T.E., Blanco, N., Tomlinson, A.J., Rowe, H.D, Houston, J., 2010. Evidence for the development of the Andean rain shadow from a Neogene isotopic record in the Atacama Desert, Chile. *Earth and Planetary Science Letters* **292**, 371–382: doi.org/10.1016/j.epsl.2010.02.004.

Retallack, G.J., 2019. *Soils of the Past. An Introduction to Paleopedology, 3rd ed*. Wiley-Blackwell, Hoboken, NJ, 559 pp.

Roy, M., Bergeron, G., La Rochelle, P., Leroueil, S., Konrad, J. M., 1995. Effets de cycles de gel-dégel sur les propriétés d'une argile sensible. *Canadian Geotechnical Journal* **32**, 725–740: doi.org/10.1139/t95-070.

Schwamborn, G., Fedorov, G., Ostanin, N., Schirrmeister, L., Andreev, A., El'gygytgyn Scientific Party, 2012. Depositional dynamics in the El'gygytgyn Crater margin: implications for the 3.6 Ma old sediment archive. *Climate of the Past* **8**, 1897–1911: doi.org/10.1139/t95-070.

Seilacher, A., 2001. Concretion morphologies reflecting diagenetic and epigenetic pathways. *Sedimentary Geology* **143**, 41–57: PII: S0037- 0738(01) 00092-6.

Silva Nieto, D., Espejo, P.M., Chernicoff, C.J., Zappettini, E.O., 2017. Hoja Geológica 3766-IV, General Acha. Provincia de La Pampa. *Boletín Servicio Geológico Minero Argentino, Instituto de Geología y Recursos Minerales* **427**, 1–52.

Tapia, A., 1935. Pilcomayo. Contribución al conocimiento de las llanuras Argentinas. *Boletín Dirección General Industria Minera* **40**, 1–124.

Techer, I., Clauer, N., Vogt, T., 2014. Origin of calcareous dust in Argentinean Pleistocene periglacial deposits traced by Sr, C and O isotopic compositions, and REE distribution. *Chemical Geology* **380**, 119–132: doi.org/10.1016/j.chemgeo.2014.04.024.

Ton-That, T., Singer, B., Mörner, N.A., Rabassa, J., 1999. Datacion de lavas basalticas por $^{40}Ar/^{39}Ar$ y geologia glacial de la Region del Lago Buenos Aires, Provincia de Santa Cruz, Argentina. *Revista Asociación Geológica Argentina* **54**, 333–352.

https://doi.org/10.1017/qua.2022.30 Published online by Cambridge University Press

Tricart, J., 1967. Le modelé des régions périglaciaires. In: Tricart, J., Cailleux, A., *Traité de Géomorphologie II*. Société d'Edition d'Enseignement Supérieur (SEDES), Paris.

Tzedakis, P.C., Andrieu, V., de Beaulieu, J.L., Crowhurst, S., Follieri, M., Hooghiemstra, H., Magri, D., *et al.*, 1997. Comparison of terrestrial and marine records of changing climate of the last 500,000 years. *Earth and Planetary Science Letters* **150**, 171–176: doi.org/10.1016/S0012-821X(97)00078-2.

Van Everdingen, R.O., 1976. Geocryological terminology. *Canadian Journal of Earth Sciences* **13**, 862–867.

Verzi, D.H., Montalvo, C.I., Vucetich, M.G., 1991. Nuevos restos de *Xenodontomys simpsoni* Kraglievich y la sistemática de los más antiguos Ctenomyinae (Rodentia, Octodontidae). *Ameghiniana* **28**, 325–331.

Viers, G., 1965. Observations sur la glaciation Quaternaire dans les Andes de Mendoza (République Argentine). *Revue Géographique des Pyrénées et du Sud-Ouest* **36**, 89–116.

Violante, R.A., Paterlini, C.M., Marcolini, S.I., Costa, I.P., Cavallotto, J.L., Laprida, C., Dragani, W., *et al.*, 2014. Chapter 6: the Argentine continental shelf: morphology, sediments, processes and evolution since the Last Glacial Maximum. In: Chiocci, F.L., Chivas, A.R. (Eds.), *Continental Shelves of the World: Their Evolution During the Last Glacio-Eustatic Cycle*. Geological Society, London, Memoirs 41, pp. 55–68.

Vogt, H., Vogt, T., Calmels, A.P., 2010. Influence of the post-Miocene tectonic activity on the geomorphology between Andes and Pampa Deprimida in the area of Provincia de La Pampa, Argentina. *Geomorphology* **121**, 152–166: doi.org/10.1016/j.geomorph.2010.03.011.

Vogt, T., 1990. Cryogenic physico-chemical precipitations: iron, silica, calcium carbonate. *Permafrost Periglacial Processes* **1**, 283–293: doi.org/10.1002/ppp.3430010308.

Vogt, T., Corte, A. E., 1996. Secondary precipitates in Pleistocene and present cryogenic environments (Mendoza Precordillera, Argentina, Transbaikalia, Siberia, and Seymour Island, Antarctica). *Sedimentology* **43**, 53–64: doi.org/10.1111/j.1365-3091.1996.tb01459.x.

Vogt, T., Larqué, P., 1998. Transformations and neoformations of clay in the cryogenic environment: examples from Transbaikalia (Siberia) and Patagonia (Argentina). *European Journal of Soil Science* **49**, 367–376: doi.org/10.1046/j.1365-2389.1998.4930367.

Vogt, T., Larqué, P., 2002. Clays and secondary minerals as permafrost indicators: examples from the circum-Baikal region. *Quaternary International* 95–96, 175–187: doi.org/10.1016/S1040-6182(02)00038-1.

Vogt, T., Calmels, A.P., Carballo, O.C., Larqué, P., 2002. Occurrence, characteristics and genesis of the duricrusts in the La Pampa plateau, Argentina. In: Faz Cano, A., Ortiz, R., Mermut A.R. (Eds.), *Sustainable Use and Management of Soils in Arid and Semiarid Regions*. Universidad de Cartagena (Espagne), v. 2, pp. 38–39.

Vogt, T., Clauer, N., Techer, I., 2018. The glaciogenic origin of the Pleistocene calcareous dust in Argentina on the basis of field, mineralogical, textural, and geochemical analyses. *Quaternary Research* **91**, 218–233: doi.org/10.1017/qua.2018.74.

Walter, H.J., Hegner, E., Diekmann, B., Kuhn, G., Rutgers van der Loeff, M., 2000. Provenance and transport of terrigenous sediment in the South Atlantic Ocean and their relations to glacial and interglacial cycles: Nd and Sr isotopic evidence. *Geochimica et Cosmochimica Acta* **64**, 3813–3827: doi.org/10.1016/S0016-7037(00)00476-2.

Washburn, A.L., 1980. *Geocryology. A Survey of Periglacial Processes and Environments*. John Wiley and Sons, New York.

Wenzens, G., 2006. Terminal moraines, outwash plains, and lake terraces in the vicinity of Lago Cardiel (49°S; Patagonia, Argentina)—evidence for Miocene Andean foreland glaciations. *Arctic, Antarctic, and Alpine Research* **38**, 276–291: doi.org/10.1657/1523-0430(2006)38[276:TMOPAL]2.0.CO;2.

Willett, C.D., Ma, K.F., Brandon, M.T., Hourigan, J.K., Christeleit, E.C., Shuster, D.L., 2020. Transient glacial incision in the Patagonian Andes from ~6 Ma to present. *Science Advances* **6**, eaay1641. https://doi.org/10.1126/sciadv.aay1641.

Williams, P.J., Smith, M.W., 1989. *The Frozen Earth. Fundamentals of Geocryology*. Cambridge University Press. Cambridge.

Zavala, C., Freije, R.H., 2001. On the understanding of aeolian sequence stratigraphy: an example from Miocene–Pliocene deposits in Patagonia, Argentina. *Rivista Italiana di Paleontologia e Stratigrafia* **107**, 251–264: doi.org/10.13130/2039-4942/5435.

https://doi.org/10.1017/qua.2022.30 Published online by Cambridge University Press